PHYSICAL REVIEW D

PARTICLES AND FIELDS

THIRD SERIES, VOL. 4, NO. 5 1 SEPTEMBER 1971

Proton-Deuteron Elastic Scattering at 1.0 GeV/c*

N. E. Booth,† C. Dolnick,‡ R. J. Esterling,§ J. Parry,‖ J. Scheid,† and D. Sherden**
The Enrico Fermi Institute and Department of Physics, The University of Chicago, Chicago, Illinois 60637
(Received 29 January 1971)

The differential cross section and polarization in p-d elastic scattering have been measured at an incident laboratory momentum of 0.99 GeV/c (kinetic energy 425 MeV) over most of the angular range. Elastic p-d scattering events from a CD_2 target were selected by angular correlation, coplanarity, and time of flight. A significant feature of the results is the large positive polarization at backward scattering angles.

I. INTRODUCTION

The study of proton-deuteron elastic scattering is of considerable interest. The deuteron is the simplest nuclear system and its interaction with nucleons can be treated from several points of view. For forward scattering, the multiple-scattering theory of Glauber[1] has been used recently to describe experimental results at high energies.[2] There is also the hope that at lower energies the three-body problem may be treated in a more rigorous way[3] than by the use of the impulse approximation.[4] At backward scattering angles, the results have been treated in terms of the baryon transfer or pickup mechanism[5] and more recently by the Reggeized nucleon-exchange process.[6]

Previous measurements of the differential cross section in p-d elastic scattering have been made at[7] 450 MeV and at a large number of other energies.[8] The only recent experiments above 100 MeV which have obtained data over most of the angular range have been performed at[9] 580 MeV and[10] 1 GeV. From the available measurements it is not clear how the pattern of the angular distribution changes with energy above about 100 MeV. However, above 1 GeV, results are now available at several energies for scattering at small momentum transfers,[11-14] and also for scattering at backward angles.[11] A compilation of all the cross-section data for nucleon-deuteron elastic scattering may be found in the recent review article by Seagrave.[8]

Measurements of the polarization (or asymmetry in the scattering of a polarized proton beam) are not nearly so extensive at energies above about 50 MeV.[15] Measurements over the entire angular range have been made at 138 MeV and 146 MeV;[16,17] and at mainly forward angles at 135, 155, 310, 419, and 544 MeV.[18-22]

We present here results of measurements of both the differential cross section and polarization at 425 MeV over the range $0.88 > \cos\theta' > -1.0$, where θ' is the scattering angle in the c.m. system.

II. EXPERIMENTAL ARRANGEMENT

The measurements of the differential cross section and polarization in p-d elastic scattering were obtained with a polarized proton beam produced at an internal target at the University of Chicago 450-MeV cyclotron.

Many of the experimental details are similar to those of an experiment on the reaction $pp \to \pi^+ d$, described by Dolnick,[23] and will not be repeated here.

The proton beam had a polarization P_B of 0.535 $\pm$ 0.025 directed vertically upwards as it emerged from the cyclotron.[24] A solenoid magnet in the experimental area was used to rotate the polarization through 90° into the horizontal plane. Scat-

tered events were detected in the vertical plane, and asymmetries were measured by running with the solenoid in one polarity, and then reversing it.

A diagram of the scintillation-counter arrangement used to detect the p-d elastically scattered events is shown in Fig. 1. The proton beam was collimated at the exit of the solenoid to remove beam halo, and was then defined by the counter T and a two-dimensional hodoscope HV. CD_2 targets were used, and the measurements were made in five separate geometries or counter combinations to cover various parts of the angular range. Details of the scintillation-counter hodoscopes (banks) $A\theta$, $A\phi$, and $B\theta$, $B\phi$ are described in Ref. 23. The veto counter shown in Fig. 1, whose location changed somewhat with the different geometries, was used to eliminate events scattered from T or from the HV hodoscope.

Details of the counter geometries used are given in Table I. The physical hodoscope geometry remained the same for geometries I, II, and III. However, for geometry I, in order to reduce the energy loss of the recoil deuteron for small proton scattering angles, a very thin CD_2 target was used, the $B\phi$ counters were not required in the electronic logic, and a helium-filled container was placed between the target and the $B\theta$ counters. In geometries I and II the proton was detected in the A bank, whereas in geometry III the proton was detected in the B bank. Data for geometries II and III were taken simultaneously and separated in the data analysis. For geometries IV and V the A and B banks were moved to accept events for which the proton was scattered in the moderately backward and very backward directions, respectively. In Fig. 1 the hodoscopes are shown in position for geometries I, II, and III (solid lines) and for geometry V (dashed lines).

In all geometries both the scattered proton and the recoil deuteron were detected. An event signal was generated in the fast electronics logic by a coincidence between T, HV, $A\theta$, $A\phi$, $B\theta$, and $B\phi$. This event signal was used to gate signals from the hodoscope counters into storage registers with a resolving time of about 20 nsec. The contents of the storage registers were strobed into an on-line computer.[25] The computer also read in the contents of an analog-to-digital converter (ADC) which was used together with time-to-height converters to measure the times of flight from counter T to the $A\theta$ and $B\theta$ counters. Usually several runs of 2–4 h each were taken for

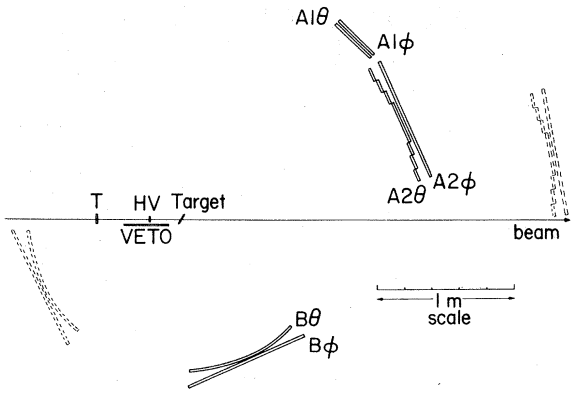

FIG. 1. Experimental arrangement for the measurement of differential cross sections and polarizations in proton-deuteron elastic scattering. The polarized proton beam impinges on the CD_2 target from the left, and is defined by the counter T and the crossed hodoscope HV. Scattered particles are detected by the counter hodoscopes $B\theta$, $B\phi$, and $A\theta$, $A\phi$. The hodoscopes are shown (solid lines) positioned for proton scattering angles less than 90° in the laboratory system. In this case scattered protons are detected in both the A and B arrays, depending upon the scattering angle. The dashed lines indicate the positions for proton scattering angles near the backward direction. The veto counter, whose position was changed slightly from one geometry to another, electronically removed events in which a particle was scattered by the HV hodoscope into the $B\theta$, $B\phi$ hodoscopes.

TABLE I. Details of geometry for proton-deuteron elastic scattering at 425 MeV.

Geometry	Defining particle	Defining bank	Lab angular range[a] (deg)	Range of $\cos\theta'$ (c.m.)	CD_2-target thickness (g cm^{-2})	Target angle[b] (deg)	Background-subtraction method[c]
I	deuteron	B	−43.5 to − 85	0.884 to 0.512	0.056	+65	fitting
II	deuteron	B	−43.5 to − 85	0.771 to 0.188	0.761	−30	fitting
III	deuteron	A	+10 to + 52	0.260 to −0.479	0.761	−30	fitting
IV	proton	B	−89.5 to −131	−0.586 to −0.898	0.761	+30	noncoplanar
V	proton	B	−133.5 to −175	−0.928 to −0.996	0.761 and 0.331	+10	noncoplanar

[a] Measured counterclockwise from the direction of the incident beam in the plane of Fig. 1.
[b] Angle between the plane of the target and the vertical measured counterclockwise in Fig. 1.
[c] The methods are described in the text.

each of the two solenoid polarities and for each geometry. In the cases where there was an overlap in c.m. angle in two different geometries, the results agreed well.

III. DATA ANALYSIS

The on-line computer was capable of doing most of the analysis and gave important information on the operation of the experiment. Single-event information was also written onto magnetic tape for a more careful future analysis.

Events due to elastic proton-deuteron scattering were separated from background events by means of three selection criteria:

(1) coplanarity of the incoming proton and the two final-state particles;

(2) angular correlation corresponding to the kinematics of p-d elastic scattering;

(3) time of flight of either the final-state proton, or deuteron, or both.

For proton laboratory scattering angles θ greater than about 90° there was little problem with background. In Fig. 2 we show the details of the analysis at a single typical scattered proton angle ($\theta = 135°$, corresponding to a proton-scattering angle in the c.m. system $\theta' = 158°$) for one of the runs. Figure 2(a) is a plot of the deviation from coplanarity ($\Delta\phi$) of the deuteron, where ϕ is the azimuthal angle with respect to the plane defined by the incident and scattered proton. Coplanarity cuts were made at the locations of the arrows. In Fig. 2(b) the dashed histogram is the time-of-flight distribution to the proton defining bin; each ADC channel corresponds to 0.3 nsec. The solid histogram is the resultant distribution after coplanarity and angular correlation cuts were made. Time-of-flight cuts were made at the locations of the arrows. Figure 2(c) shows (dashed histogram) the angular-correlation ($\Delta\theta$) distribution before any coplanarity or time-of-flight cuts were made, and (solid histogram) after these cuts were made. The quantity $\Delta\theta$ is the difference between the observed deuteron lab angle, and the angle computed kinematically from the lab angle of the coincident proton. The dots show the angular correlation of events outside the $\Delta\phi$ cuts of Fig. 2(a), but inside the time-of-flight cuts. These events have been normalized to the solid histogram of Fig. 2(c) in the region *outside* the arrows. The number of elastic events was obtained by subtracting the dots from the solid histogram in the region between the arrows. This type of analysis was carried out for data taken with geometries IV and V.

In the $\Delta\theta$ distribution of Fig. 2(c) there is no evidence for a peak due to quasifree p-d scattering from the carbon component of the CD_2 target. In other experiments where we have measured π-p scattering[26] and p-p scattering[24] from targets containing complex nuclei, we have observed quasifree peaks in both the $\Delta\phi$ and $\Delta\theta$ distributions. However, the quasifree peaks are at least a factor of 10 wider in both plots, and the method of analysis used here is able to reject events from

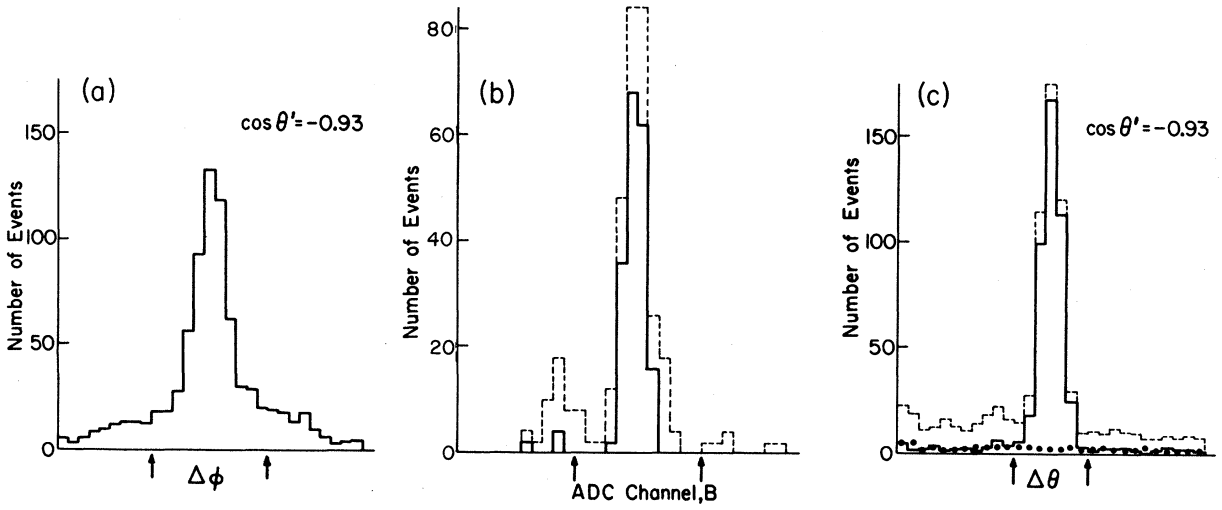

FIG. 2. Histograms showing the method of event selection in a typical case: (a) A plot of $\Delta\phi$, the deviation from coplanarity, for detected events. The arrows show where coplanarity cuts were made. (b) Time-of-flight spectrum to a proton-detecting counter. The dashed spectrum is for all events; the solid spectrum is for those events lying inside the ϕ and θ cuts. (c) Plots of angular correlation. The dashed histogram is for all events; the solid histogram is for those events lying within the ϕ and time-of-flight cuts; the dots represent the normalized distribution for those events lying outside the ϕ cuts.

this source. We verified this in the present experiment by observing p-p scattering from CH_2 and C targets. We conclude that either the cross section for quasifree p-d scattering is relatively smaller, or the correlation is smeared out even more for bound deuterons as compared to bound protons.

A more serious problem arises at proton scattering angles less than about 90° in the laboratory system. Here the background from deuteron break-up or quasifree p-p scattering from the deuteron becomes severe. Geometries I–III were efficient in detecting a proton in the A banks in coincidence with a proton in the B bank. The two final-state protons produced when deuteron break-up occurs are also partially correlated in angle, both in θ and in ϕ. A further complication arises at about 50° in the laboratory system where the proton and deuteron from p-d elastic scattering come out at equal angles to the beam direction. In the absence of time-of-flight information to provide particle identification, there is an ambiguity in the c.m. scattering angle. We found that time-of-flight cuts, particularly on the deuteron, removed most of the background. Figure 3 shows two typical time-of-flight spectra taken in geometries II and III for a B-bank counter at a laboratory angle of −55° and an A-bank counter at +46°. The large peak in each of the heavy-lined spectra is due to protons from quasielastic p-p scattering in the deuteron. The smaller peak at larger ADC-channel number is in each case due to deuterons. When θ and ϕ cuts kinematically appropriate to requiring protons in the B bank and deuterons in the A bank are imposed, we obtain the thin-lined histograms. When θ and ϕ cuts appropriate for protons in the A bank and deuterons in the B bank are made, the dashed histograms are obtained. From the latter two sets of histograms, it is straightforward to see where to put the time-of-flight cuts so that no events of interest are lost and so that as much background as possible is rejected. Since the times of flight of the protons from p-d elastic and from p-p quasielastic scattering are so similar, in most cases cuts were made only to select deuterons. After the time-of-flight cuts were made, the $\Delta\phi$ and $\Delta\theta$ distributions were made again and the ϕ and θ cuts adjusted. In most cases the resulting $\Delta\theta$ distributions were similar to that of Fig. 2(c) and rarely was the background under the elastic peak more than 10% of the peak.

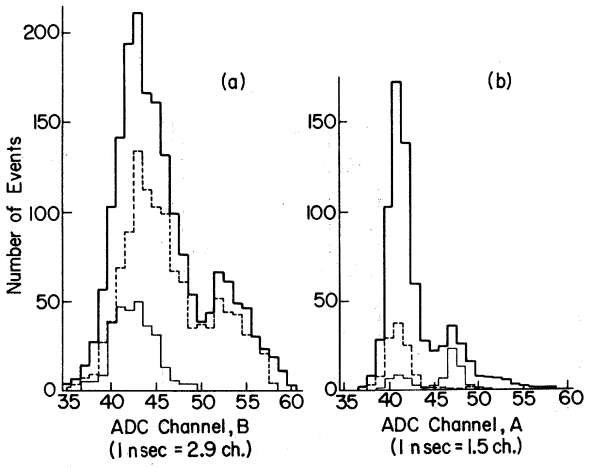

FIG. 3. Typical time spectra for proton laboratory angles less than 90°: (a) Time spectra for a counter in the B hodoscope. (b) Time spectra for a counter in the A hodoscope. In each case the thick-lined histograms are for all events; the dashed-line histograms result when θ cuts corresponding to protons in A and deuterons in B are imposed; the thin-line histograms result when θ cuts corresponding to protons in B and deuterons in A are imposed.

Although we tried computing the results by means of the background subtraction method based on the angular correlation distributions of the noncoplanar events [as used in Fig. 2(c)], this method is incorrect when the background is highly correlated or when more than one source of background is present. This method assumes that the $\Delta\theta$ distributions of the background events have the same shape for events inside and outside the ϕ cuts. This is not true for quasielastic p-p scattering from deuterium where events inside the ϕ cuts tend to be more highly correlated in θ than those outside. Consequently, the shapes of the two background distributions are different inside and outside the ϕ cuts, resulting in different $\Delta\theta$ distributions. Hence polynomial fits to the coplanar background outside the θ cuts were used to determine the background inside the θ cuts. In spite of the objections to the first method, the results of the two methods agreed to within statistical errors except in a few cases where one of the methods was obviously incorrect.

Once the number of elastic events was found for each defining bin and sign of solenoid polarity, rates per incident beam particle were computed. If R_+ (R_-) is the scattering rate with the incident-proton spin parallel (antiparallel) to $\vec{k}_i \times \vec{k}_f$ ($\vec{k}_i$ and $\vec{k}_f$ are the c.m. momenta of the incident and scattered proton, respectively), then the asymmetry ϵ and polarization P are given by

$$\frac{R_+ - R_-}{R_+ + R_-} = \epsilon = PP_B.$$

The differential cross section is proportional to $\frac{1}{2}(R_+ + R_-)$.

Solid angles were computed with the aid of a Monte Carlo program. In computing the differen-

TABLE II. Cross sections and polarizations for proton-deuteron elastic scattering at 1.0 GeV/c.

Geometry[a]	$\cos\theta'$ (c.m.)	$-t$ (GeV/c)^2	$d\sigma(\theta')/d\Omega$ (μb/sr)	$P(\theta')$
I	0.884	0.084	...	0.636± 0.052
	0.850	0.108	...	0.450± 0.042
	0.813	0.135	...	0.260± 0.040
I, II	0.771	0.165	834 ± 63	0.214± 0.026
	0.725	0.199	459 ± 35	0.102± 0.020
	0.677	0.233	293 ± 23	−0.112± 0.018
	0.625	0.271	249 ± 12	−0.174± 0.020
	0.570	0.311	176 ± 10	−0.323± 0.026
	0.512	0.353	125 ± 7	−0.451± 0.033
II	0.451	0.397	...	−0.566± 0.076
	0.388	0.442	74.9± 4.9	−0.537± 0.042
	0.324	0.488	69.5± 4.5	−0.501± 0.047
III	0.260	0.535	66.4± 3.5	−0.400± 0.057
II	0.257	0.537	61.7± 4.0	−0.421± 0.049
III	0.205	0.574	60.8± 4.3	−0.402± 0.074
II	0.188	0.587	...	−0.480± 0.051
III	0.161	0.606	66.4± 4.7	−0.514± 0.076
	0.117	0.638	54.8± 4.1	−0.446± 0.084
	0.072	0.670	61.7± 4.3	−0.497± 0.072
	0.027	0.703	59.8± 4.1	−0.285± 0.071
	−0.019	0.736	54.7± 3.8	−0.198± 0.075
	−0.064	0.769	54.3± 3.8	−0.371± 0.074
	−0.171	0.846	44.4± 3.1	−0.178± 0.077
	−0.217	0.879	44.9± 3.1	−0.084± 0.075
	−0.262	0.912	41.8± 2.9	−0.110± 0.075
	−0.307	0.944	39.7± 2.9	−0.056± 0.082
	−0.351	0.976	37.6± 2.8	−0.020± 0.079
	−0.395	1.008	32.2± 2.4	−0.134± 0.090
	−0.437	1.038	32.3± 2.5	0.146± 0.093
	−0.479	1.068	30.8± 2.4	0.135± 0.078
IV	−0.586	1.146	28.0± 2.0	0.269± 0.077
	−0.637	1.183	36.5± 2.4	0.290± 0.064
	−0.683	1.216	38.6± 2.6	0.322± 0.066
	−0.725	1.246	46.1± 3.0	0.437± 0.059
	−0.762	1.273	49.7± 3.4	0.349± 0.060
	−0.796	1.297	64.9± 4.1	0.301± 0.051
	−0.826	1.319	77.3± 5.0	0.248± 0.047
	−0.852	1.338	88.1± 5.6	0.322± 0.046
	−0.875	1.355	98.3± 6.3	0.241± 0.043
	−0.898	1.371	103.4± 6.4	0.164± 0.038
V	−0.928	1.393	131 ± 10	0.125± 0.055
	−0.942	1.403	140 ± 10	0.152± 0.055
	−0.954	1.412	144 ± 11	
	−0.964	1.419	151 ± 11	0.126± 0.032
	−0.973	1.425	168 ± 13	
	−0.986	1.435	176 ± 13	0.076± 0.036
	−0.996	1.442	...	0.038± 0.059
	−1.000	1.445	190[b] ± 10[b]	

[a]Details of the different geometries are given in the text and in Table I.
[b]Value obtained by semilogarithmic extrapolation.

tial cross sections. nuclear absorption corrections of between 3% and 12% were applied for loss of beam particles in the *HV* hodoscope and target, and loss of final-state particles in the target, air, and θ and ϕ counters. In making these corrections we made use of the calculations of Measday and Richard-Serre,[27] and of deuteron absorption cross sections of Millburn *et al.*[28]

At extreme forward and backward scattering angles where the deuteron and proton, respectively, have very low range, we rejected the cross-section measurements, but we believe the polarization measurements to be reliable. Also, in a few cases, the elastic peak in the $\Delta\theta$ plot was close to the edge of a counter bank and cross-section results were rejected because some of the events may have been lost due to the geometry.

IV. RESULTS

The results for the differential cross sections in the c.m. system and polarizations are given in Table II and in Fig. 4. For convenience we also tabulate $-t = 2q^2(1-\cos\theta')$, where q is the momentum in the c.m. system. The errors in the cross sections include the statistical error and errors in the target thicknesses (±5%) and solid angles (typically ±4%). In addition, there is a ±10% normalization error due to uncertainties in beam monitoring and to some extent in the nuclear absorption corrections. The polarization errors given are statistical; in addition, there is a ±5% normalization error due to uncertainties in beam polarization and beam monitoring.

The differential cross section is similar in shape to that measured at 580 MeV by Vincent *et al.*[9]; the forward peak, the change in slope at about $\cos\theta' = 0.4$, and the backward peak are qualitatively the same at both energies. The earlier data of Crewe *et al.*[7] at 450 MeV do not indicate such an abrupt change in slope. This change in slope occurs at a value of the momentum-transfer variable $-t \approx 0.4$ (GeV/c)^2. In recent data at 9.7 and 12.8 GeV/c, a sharp break occurs at this same value of $-t$.[14] This break has been interpreted in terms of successive scatterings from the two nucleons in the deuteron.[2] Not only has the fact that there is an admixture of D state in the deuteron been included in the calculations, but also more recently Franco and Glauber[29] have included the spin effects in considerable detail.

The polarizations are remarkably similar to the results of Postma and Wilson[17] and Poulet *et al.*[18] at about 140 MeV, except that in our data there is perhaps an indication of additional structure near $\cos\theta' = 0.4$. Also, we observe larger polarizations near the backward direction. It is interesting that near the backward direction, the polarization is maximum near the same angle at which there is a minimum of the differential cross section. We also note that the negative-polarization maximum and possible additional structure occur at the same angle as the abrupt change in slope of the differential cross section near $\cos\theta' = 0.4$. We have not attempted to fit the data at small values of $-t$ with the model of Franco and Glauber[29] which is the most recent relevant model. The possibility of having polarized deuteron targets[30] means that measurements of the tensor polarization in p-d elastic scattering are also possible and the first results are now available.[31] These data taken together should provide a good test of the model of Franco and Glauber. We also hope that the results at backward angles will stimulate some theoretical work on the spin effects in baryon exchange.

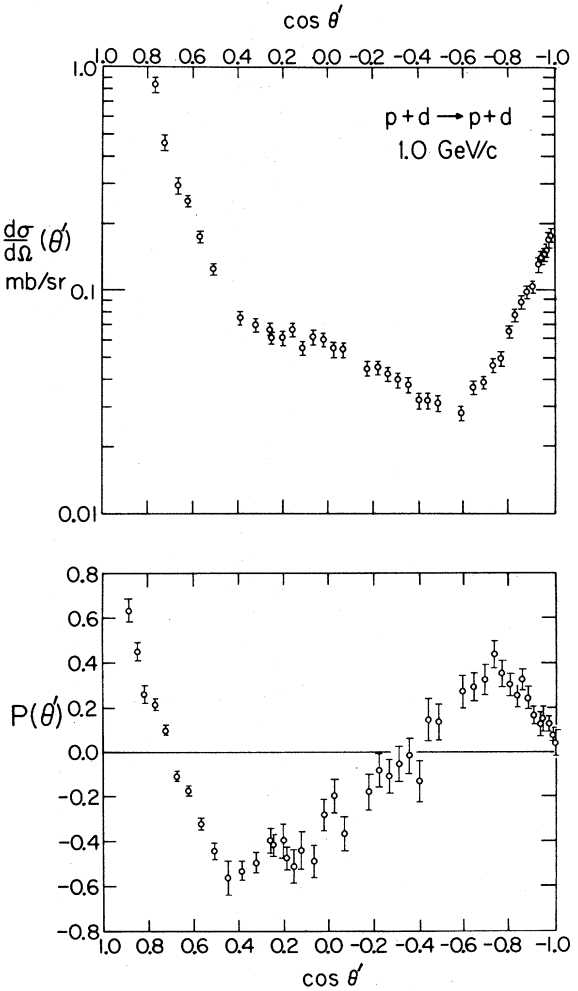

FIG. 4. Differential cross section and polarization for proton-deuteron elastic scattering at 425 MeV.

ACKNOWLEDGMENTS

We wish to thank A. Beretvas and P. Kwiatkowski for assistance during the preparation and running of the experiment. We also thank H. Hinterberger and the crew of the Chicago cyclotron, and R. Wilberg, T. Nunamaker, and R. Norton for the design and construction of much of the apparatus.

---

*Research supported by the National Science Foundation.

†Present address: Nuclear Physics Laboratory, Oxford University, Oxford, England.

‡Present address: National Accelerator Laboratory, Batavia, Ill. 60510.

§Present address: Rutherford High Energy Laboratory, Chilton, Didcot, Berks., England.

‖Present address: Computer Based Education Research Laboratory, University of Illinois, Urbana, Ill. 61801.

**Present address: SLAC, Stanford University, Stanford, Calif. 94305.

[1]R. J. Glauber, in *Lectures in Theoretical Physics*, edited by W. E. Brittin and L. G. Dunham (Interscience, New York, 1959), Vol. I, p. 315.

[2]V. Franco and R. J. Glauber, Phys. Rev. 142, 1195 (1966); V. Franco, Phys. Rev. Letters 16, 944 (1966); V. Franco and E. Coleman, *ibid.* 17, 827 (1966).

[3]H. P. Noyes, Phys. Rev. Letters 23, 1201 (1969); 24, 493 (E) (1970); 25, 321 (1970).

[4]G. F. Chew and G. C. Wick, Phys. Rev. 85, 636 (1952).

[5]R. Serber, Phys. Rev. 72, 1008 (1947); G. F. Chew and M. L. Goldberger, *ibid.* 77, 470 (1950); J. N. Chahoud and G. Russo, Nuovo Cimento 49A, 206 (1967).

[6]A. K. Kerman and L. S. Kisslinger, Phys. Rev. 180, 1483 (1969).

[7]A. V. Crewe, B. Ledley, E. Lillethun, S. Marcowitz, and L. G. Pondrom, Phys. Rev. 114, 1361 (1959).

[8]J. D. Seagrave, in *Proceedings of the First International Conference on the Three-Body Problem in Nuclear and Particle Physics*, edited by J. S. C. McKee and P. M. Rolph (North-Holland, Amsterdam, 1970).

[9]J. S. Vincent, W. K. Roberts, E. T. Boschitz, L. S. Kisslinger, K. Gotow, P. C. Gugelot, C. F. Perdrisat, L. W. Swenson, and J. R. Priest, Phys. Rev. Letters 24, 236 (1970).

[10]G. W. Bennett, J. K. Friedes, H. Palevsky, R. J. Sutter, G. J. Igo, W. D. Simpson, G. C. Phillips, R. L. Stearns, and D. M. Corley, Phys. Rev. Letters 19, 387 (1967).

[11]E. Coleman, R. M. Heinz, O. E. Overseth, and D. E. Pellett, Phys. Rev. Letters 16, 761 (1966).

[12]L. S. Zolin, L. F. Kirillova, Lu Ch'ing-Ch'iang, V. A. Nikitin, V. S. Pantuev, V. A. Sviridov, L. N. Strunov, M. N. Khachaturyan, M. G. Shafranova, Z. Korbel, L. Rob, P. Devinski, Z. Zlatanov, P. Markov, L. Khristov, Kh. Chernev, N. Dalkhazhav, and D. Tuvdendorzh, Zh. Eksperim. i Teor. Fiz. Pis'ma v Redaktsiyu 3, 15 (1966) [Soviet Phys. JETP Letters 3, 8 (1966)]; see also Ref. 8.

[13]J. V. Allaby, A. N. Diddens, R. J. Glauber, A. Klovning, O. Kofoed-Hansen, E. J. Sacharidis, K. Schlupmann, A. M. Thorndike, and A. M. Wetherell, Phys. Letters 30B, 549 (1969); G. Bellettini, G. Cocconi, A. N. Diddens, E. Lillethun, G. Matthiae, J. P. Scanlon, and A. M. Wetherell, *ibid.* 19, 341 (1965).

[14]F. Bradamante, G. Fidecaro, M. Fidecaro, M. Giorgi, P. Palazzi, A. Penzo, L. Piemontese, F. Sauli, P. Schiavon, and A. Vascotto, Phys. Letters 32B, 303 (1970).

[15]For a review of polarization measurements in nucleon-deuteron scattering, see W. Haeberli, in *Proceedings of the First International Conference on the Three-Body Problem in Nuclear and Particle Physics*, edited by J. S. C. McKee and P. M. Rolph, Ref. 8.

[16]M. Poulet, A. Michalowicz, Y. LeGuen, K. Kuroda, D. Cronenberger, and G. Coignet, J. Phys. Radium 26, 1229 (1965).

[17]H. Postma and R. Wilson, Phys. Rev. 121, 1229 (1961).

[18]M. Poulet, A. Michalowicz, K. Kuroda, and D. Cronenberger, Nucl. Phys. A99, 442 (1967).

[19]K. Kuroda, A. Michalowicz, and M. Poulet, Nucl. Phys. 88, 33 (1966).

[20]J. Marshall, L. Marshall, D. Nagle, and W. Skolnik, Phys. Rev. 95, 1020 (1954).

[21]S. M. Marcowitz, Phys. Rev. 120, 891 (1960).

[22]K. Gotow (private communication on results of the authors of Ref. 9).

[23]C. L. Dolnick, Nucl. Phys. B22, 461 (1970).

[24]A. Beretvas, Phys. Rev. 171, 1392 (1968).

[25]An EMR-6040, manufactured by Electro Mechanical Research, Inc.

[26]R. E. Hill, N. E. Booth, R. J. Esterling, S. Suwa, and A. Yokosawa, Phys. Rev. D 1, 729 (1970).

[27]D. F. Measday and C. Richard-Serre, Nucl. Instr. Methods 76, 45 (1969).

[28]G. P. Millburn, W. Birnbaum, W. E. Crandall, and L. Schecter, Phys. Rev. 95, 1268 (1954).

[29]V. Franco and R. J. Glauber, Phys. Rev. Letters 22, 370 (1969).

[30]M. Borghini, invited paper presented at the Sixième Rencontre de Moriond sur les Interactions Electromagnétiques, 1971 (unpublished).

[31]M. G. Albrow, M. Borghini, B. Bosnjakovic, F. C. Erne, Y. Kimura, J. P. Lagnaux, J. C. Sens, and F. Udo, Phys. Letters 35B, 247 (1971).